Increase of Regression Speed of Combustion through Oxidizer Doping

Florin Mingireanu[a,b], Lucian P. Georgescu[b], Gabriel Murariu[b], Ionut Mocanu[b],
Marius Stoia-Djeska[a,e], Nicolae Jula[c,d]

[a]*Romanian Space Agency,*
str. Mendeleev, 21-25, sector 1, Bucharest, 010362, Romania, e-mail: florin.mingireanu@rosa.ro
[b]*University "Dunarea de Jos" of Galati, Romania,*
European Center of Excellence for the Environment (ECEE), e-mail: gabriel.murariu@ugal.ro
[c]*Tehnical Military Academy,*
Bvd. George Cosbuc, 81-83, sector 5, Bucuresti, Romania, e-mail: nicolae.jula@gmail.com
[d]*University of South-East Europe Lumina,*
Sos. Colentina, 64b, sector 2, Bucuresti, Romania
[e]*Politehnica University of Bucharest (UPB),*
Splaiul Independentei, 313, sector 6, Bucuresti, Romania, e-mail: marius.stoia@rosa.ro

This paper presents an innovative method to increase the regression speed of a solid fuel grain by using oxidizer doping. The results obtained on a propulsion application showing the performance parameters as an output of a numerical model are provided. Two models are given that predict the regression speed increase for embedding wires and for oxidizer doping with a factor of ~ 2 to 3. Also, it is shown that this increase of the regression speed by using a low oxidizer doping percentage, which is based on the assumption that at a higher doping rate the combustion instabilities, can lead to detonations. Next, a thermochemical model for the combustion within the oxidizer doping model is afforded. For this model, the burn is assumed to take place around the surface of each of the oxidizer particles, being composed of two different burning processes: one is the burning on the surface of the solid fuel grain and the other is the burning between the solid fuel and the solid oxidizer. For a non-doped fuel grain, the burning takes place only on the surface of the fuel grain. Finally, a potential application of such propulsion units to small satellite launchers is presented, and a case study of such a vehicle intended to place a 50 kg payload on a low earth orbit (300 to 500 km altitude) is described. The modelling proposed is based on the assumption that the use of solid methane makes this launcher environmentally friendly.

Keywords: combustion, doping, oxidizer, regression, ballistics.

INTRODUCTION

Hybrid rocket engines/motors are alternative propulsion for future aerospace vehicles. A direct hybrid rocket motor uses a solid fuel and a liquid oxidizer while an indirect hybrid rocket motor uses a solid oxidizer and a liquid fuel. In this paper we are focusing on a solid-methane- based direct hybrid rocket motor (SM-HRM).

Hybrids have been investigated for a long time, with first recorded works by S.P. Korolev and M.K. Tikhonravov using a mixture of gaseoline, collophonium (gelled gasoline) and liquid oxygen on a 500 N thrust motor [1].

This motor was tested in flight on August 17, 1933, propelling the rocket at ~ 500 m altitude [2]. Hybrid engines have an advantage over liquid rocket motors: the former use half of the plumbing since pipes are needed only for the oxidizer installation. In addition, the safety in operation of a hybrid engine is higher than that of a solid rocket motor since a hybrid can be shut down by controlling the oxidizer inflow.

Regarding the SM-HRM, it is worth noting that V.P. Glushko and G.E. Langemak were first to consider methane as a possible rocket fuel in a book written 74 years ago [3].

This was followed by massive rocket research and developments in Russia leading to the cutting edge technology being developed in the subsequent years [3, 4].

However, at that time the utilization of methane (as well as hydrogen) was not given enough consideration because of its low density. The priority was given to the development of military type boosters using storable propellants and, hence, methane/hydrogen was not in the focus of attention in major scientific research in the field of rocket production.

For civilian applications, methane has certain advantages in comparison with kerosene, as the following:

– Higher energy density – up to 25% and higher payload assuming the same initial mass;

– Absence of carbon black formation;

– Better chamber cooling: methane can take up as much as twice more heat than kerosene;

– Safer from ecological point of view; combustion products are more ecologically friendly;

– Similar liquefying temperatures with oxygen allows for simpler constructive designs, which leads to a cheaper overall booster and smaller initial mass;

– Cheaper than kerosene;

– Large resources available worldwide.

In the present paper a novel regression speed increasing technique is proposed based on using a solid oxidizer within the solid fuel grain (e.g., solid methane).

A basic hybrid rocket motor schematics was outlined in earlier works [5–9]. In the present paper the same general schematics is considered as that in Fig. 1.
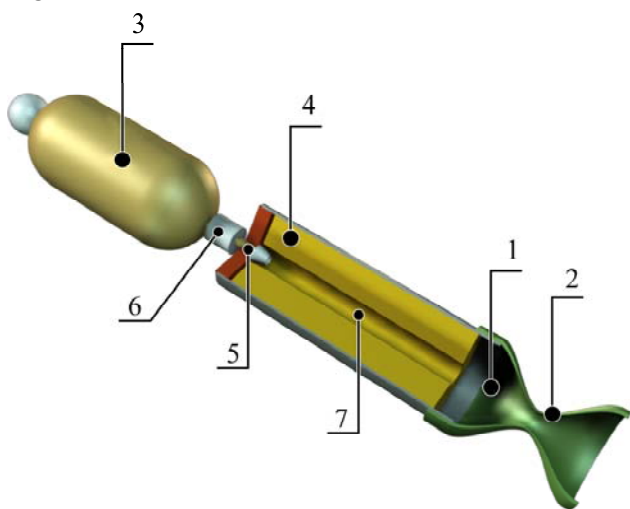

Fig. 1. Hybrid rocket engine structure based on S.P. Korolev initial design [4–8]. 1 – Combustion chamber; 2 – Nozzle; 3 – Oxidizer tank; 4 – Fuel grain; 5 – Injector valve; 6 – Head of injector valve; 7 – Burning port.

An important detail is that in our case the fuel grain is not PVC or other plastic material but frozen methane.

As for the oxidizer, it is proposed to use liquid oxygen (LOX) injected from the oxidizer tank at a constant pressure by using a turbo-pump unit. The pump unit is not represented (for the sake of simplicity) in Fig. 1. However, the unit should be installed in between the oxidizer tank and the injector and should be powered either by a separate power unit or by a portion of exhaust gases of the hybrid motor itself.

The aim of the present study is to address a major drawback of hybrids, which is a low regression speed [10, 11]. A solution is suggested to increase the regression speed by doping the fuel with solid oxidizer powder. By this doping, the regression speed can increase by a factor of 2 to 3 or even more depending on the doping solid oxidizer that is being used. The idea to add oxidizer doping is somewhat similar to the idea to add additives to liquid rocket motors in order to increase their performance [12]. In both cases the added doping (additive) increases the overall performance of the rocket motor without changing the initial fuel/oxidizer combination.

While a vast majority of hybrid rocket motors use non-cryogenic, low performance oxidizer/fuel combinations, in the present paper a cryogenic higher performance combination by using solid methane and liquid oxygen is considered. Solid methane is also well suited to oxidizer doping, which can lead to a further performance growth by increasing the regression speed rate. Several simulations have been performed showing results that are encouraging and justify further experimental work in the direction of oxidizer doping and cryogenic fuel/oxidizer combinations.

I. THERMOCHEMISTRY OF FROZEN METHANE AND INTERNAL BALLISTIC MODEL

The model proposed here follows basic internal ballistics procedures as outlined in reference works [8, 13, 14]. It is guided by the assumption of usage of a high performance injector based on swirling technology [15]. This type of an injector ensures a better "washing" of a solid fuel surface by liquid oxygen.

In addition, the performance assessment in the present paper comes from a previous work on cryogenic hybrid rocket motors [16].

The model discussed here rises from the assumption that solid methane has the same caloric power as liquid methane, but a different (higher) density. It is also supposed that the burning takes place only on the surface of the solid fuel grain within a thin layer of vaporized fuel.

According to the NIST (National Institute of Standard and Technology – federal technology agency of the US that works with industry to develop and apply technology, measurements, and standards) chemistry database, methane has a triple point at around $p = 0,1169$ atm and $T = 90$K. Since during the operation of the motor the pressure and temperature conditions are not under the above triple point values, it is possible to say that sublimation does not take place and, hence, methane suffers a three-phase transformation:

$$solid \rightarrow liquid \rightarrow gas.$$
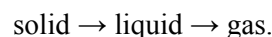
During the combustion there will be a liquid methane layer on the surface of the solid methane grain. This liquid layer vaporizes and interacts with the oxidizer burning inside the combustion chamber.

Transformations from solid to liquid and from liquid to gas state require an amount of energy equal to the sum of fusion and vaporization enthalpies.

The main thermo-chemical relation considered in the present work is this:

$$\sum_R n_i(h_f + \Delta h)_i = \sum_P n_e(h_f + \Delta h)_e \qquad (1)$$

where Δh denotes a change in enthalpy from a reference temperature, typically 298K. Here it is assumed that in the beginning the reactants are at an initial temperature equal to the reference temperature, and, hence, the left-hand-side Δh terms are all equal to zero. Using the conservation of mass in equation (1) and the values for enthalpies that can be found in the NIST Chemistry web-book one can compute the adiabatic flame temperature for certain reactants and products of reaction. The adiabatic flame temperature assumes no heat is emitted into the environment, and the chemical composition of products is maintained constant throughout the reaction. These conditions are considered to be in chemical and thermal equilibrium; under these conditions the adiabatic flame temperature is the highest one that can be obtained with certain reactants. Moreover, the adiabatic flame temperature is reached for stoichiometric ratios of the reactants mixture.

Thermo-chemically speaking, there are the following relations for the temperature and pressure in the critical section of the nozzle:

$$T^* = \frac{T_0}{1+\frac{k-1}{2}},$$

$$\qquad (2)$$

$$p^* = \frac{p_0}{[1+\frac{k-1}{2}]^{\frac{k}{k-1}}} \qquad (3)$$

where k is the ratio of specific heats at a constant volume and constant pressure, respectively, and the physical quantities with subscript 0 are measured inside the burning chamber. Also the specific impulse (4), usually abbreviated Isp, and the characteristic velocity (5) have the following thermochemical formulations according to reference [3]:

$$I_{sp} = \frac{1}{g}\sqrt{2T_0 \frac{R'}{M}(\frac{k}{k-1})[1-(\frac{p_e}{p_0})^{\frac{k-1}{k}}]}, \qquad (4)$$

$$c^* = \sqrt{\frac{(R'/M)T_0}{k(\frac{2}{k+1})^{\frac{k+1}{k-1}}}}. \qquad (5)$$

In the present investigation the CPROPEP thermo chemical software package has been used and the obtained results described herein have been also validated by the authors' custom written software based on the above thermo chemical relations. The main assumptions both for CPROPEP and for the custom written thermo chemical applications are:
- One-dimensional flow with regard to the continuity, energy and momentum equations;
- Zero flow velocity at the nozzle inlet;
- Complete and adiabatic combustion;
- Isentropic expansion in the nozzle;
- Homogeneous mixing of the reactants and products;
- Ideal-gas law applied;
- Zero temperature lag and velocity lag of the condensed-phase products.

It was noticed that a 340 s I_{sp} is obtained for the mass ratio of 25% methane and 75% liquid oxygen, at a chamber pressure of 251 atm and a temperature of 3626K. These pressure and temperature are obviously too high for any practical design; but the results imply a great potential of methane for a hybrid rocket motor. From the thermo-chemical point of view, it is possible to re-design the motor for a lower pressure and temperature, however, the I_{sp} will also decrease. For example, maintaining the mass ratio of 25% methane and 75% liquid oxygen, for a pressure of 100 atm and a temperature of 3531K, the I_{sp} of 320 s is obtained, which is rather high performance compared with that of similar systems. It is worth noting here that for all the above numerical results the shifting equilibrium was used but not frozen equilibrium. This is because the authors of the present study want their ideas to be valid for large hybrid rocket motors where nozzles are large enough, and the combustion product composition does not remain constant throughout the flow through the nozzle. If it is necessary to obtain numerical results for smaller rocket motors (e.g. hobby scale hybrid rocket motors), then one could use the frozen equilibrium that assumes that the composition of the combustion products does not change throughout the flow through the nozzle.

Figure 2 depicts the dependence of the I_{sp} on the mass ratio between methane and liquid oxygen. It can be seen that the peak performance is obtained near the ratio of oxidizer to fuel (O/F) equal to 3.
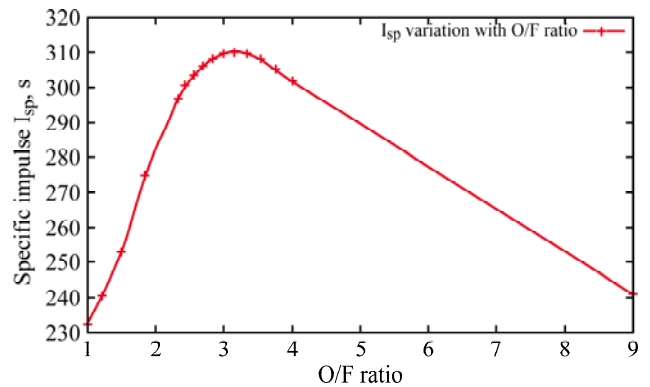

Fig. 2. I_{sp} variation with O/F ratio.

Figure 3 shows the dependence of temperature on the O/F ratio for a fixed pressure in the combustion chamber, with methane as fuel and liquid oxygen as an oxidizer. In this case, the maximum temperature is obtained for an O/F ratio of 3:4. The temperature is influenced strongly by the O/F ratio at the beginning; hence, the temperature increases sharply with

the increase of the O/F ratio until O/F reaches a value between 3 and 4. After reaching the maximum the temperature decreases slightly with a further increase of the O/F ratio.
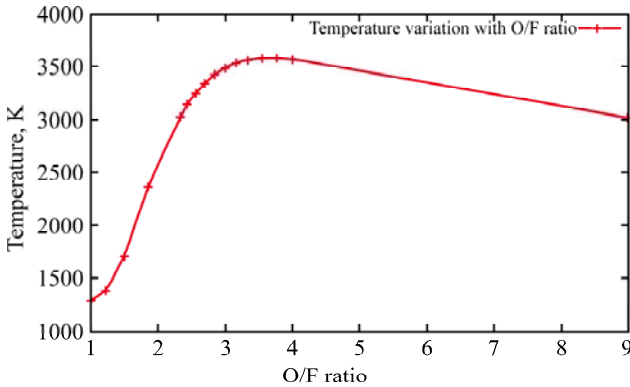

Fig. 3. Temperature variation with O/F ratio.

Figure 4 presents the variation of combustion temperature with pressure: the higher the pressure, the higher the temperature.

However, for a fixed O/F ratio, an increase of pressure in the combustion chamber leads to an increase in temperature, which, in turn, may create constructive difficulties. Hence, a variation of temperature with pressure for a fixed O/F ratio is also needed. The O/F ratio ~ 3 was chosen, that is, the same value as used before when the I_{sp} was presented as a function of pressure.

It was noticed that temperatures as high as 3900K can be reached if one increases the pressure up to 180 atm and I_{sp} approaches a value of 330 seconds.
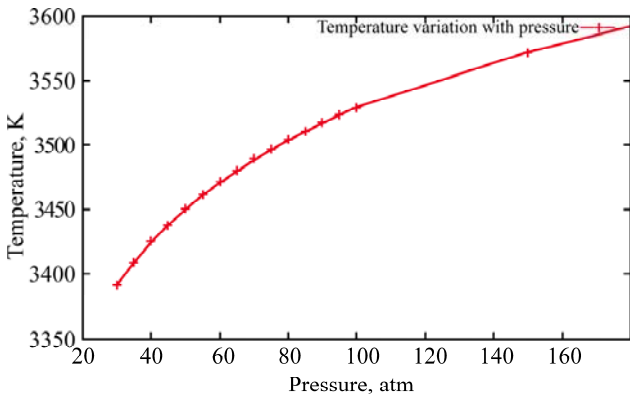

Fig. 4. Temperature variating with pressure.

Table. Comparison of performance of various O/F pairs

O/F pair	I_{sp} (s)
LOX/methane	225.2
Nitrate acid/methane	195
Oxychlorine trifluoride/methane	206
Oxygen difluoride/methane	254

Table shows data on comparing performance, which, in fact, basically demonstrates that the I_{sp} is obtained at 100 atm for various oxidizers used in combination with methane at ideal (stoichiometric) chemical ratios.

II. OXIDIZER DOPING MODEL. NUMERICAL RESULTS

Hybrids have two main drawbacks when compared to solid and liquid rocket motors:
– combustion inefficiency;
– low regression rate.

In a typical hybrid rocket motor the combustion efficiency is highly dependent on the degree of the mixture of an oxidizer and vaporized solid fuel before the oxidizer has a chance to leave the combustion chamber through the nozzle. This is the main reason for which typical hybrids are longer than typical solid rocket motors. In addition to making the burning chamber longer, designers also try to increase the burning surface (interaction surface) between the oxidizer and the fuel by using various burning port geometries (e.g.: star shape). In order to increase the regression speed, it is proposed to use the method of weak oxidizer doping of the solid fuel as outlined in [5]. Weak oxidizer doping means mixing of a small percentage of a solid oxidizer (powder) in the total mass of a solid fuel grain. Typical percentage is considered to be 3–6%, so, the doping is weak. Typical microstructure of such a fuel grain is shown in Fig. 5, where the oxidizer particles are separated from each other by more than 100 radii.
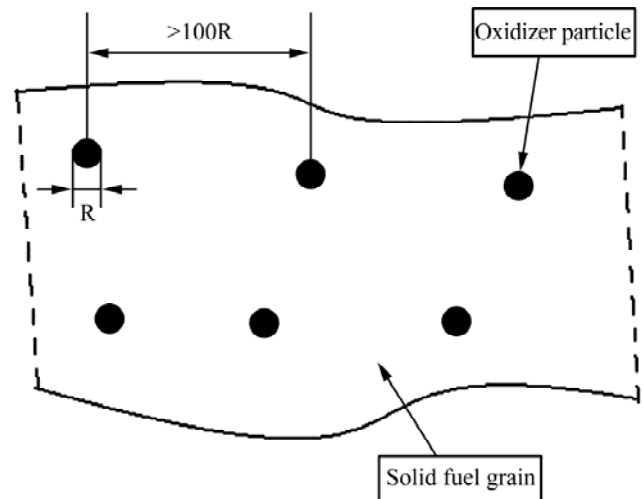

Fig. 5. Oxidizer doping.

The burn progresses from the surface of the solid fuel towards the interior. On the surface of the fuel there are only few oxidizer particles and the rest of the surface is clear fuel. If we assume that, on average, each oxidizer particle has a mass m_k, then the fuel that burns using this quantity of the oxidizer is m_x where

$$m_x = \varphi m_k, \tag{6}$$

with ϕ being the stoichiometric ratio O/F for the specific pair used. Using (6) it is convenient to deter-

mine the average volume of fuel around a given oxidizer particle that contains the needed quantity of fuel for it to be completely burnt by the interaction with the oxidizer particle:

$$V = \varphi m_k / \rho_f. \tag{7}$$

The next step is to obtain a regression speed relation for a given fuel weakly doped with an oxidizer. In the present paper the doping mass fraction is ε.

The fuel grain has a cylindrical geometry, with the burning port having the radius r.

Let's consider an infinitesimal thickness layer dr.

The total amount of fuel contained in this layer, considering that there is no oxidizer doping, is given by the following relation:

$$dm_f = \rho_f 2\pi r L dr. \tag{8}$$

The total amount of an oxidizer, considering the doping mass fraction ε, is given by:

$$dm_o^* = \varepsilon \rho_f 2\pi r L dr. \tag{9}$$

The total amount of fuel that can be oxidized by the dm_o^* oxidant is as follows:

$$dm_{fo}^* = \varepsilon\varphi\rho_f 2\pi r L dr. \tag{10}$$

The rest of the fuel that would be left non-oxidized by the solid doping oxidizer is:

$$dm_f = \rho_f 2\pi r L dr (1-\varepsilon\varphi). \tag{11}$$

The mixture of the dm_o^* fuel and dm_{fo}^* oxidizer behaves like a solid fuel:

$$\dot{r}_s = cp^\upsilon, \tag{12}$$

where $\dot{r}_s$ is the burning rate of the solid fuel. Moreover, the dm_f fuel burns with the liquid oxidizer (N_2O) as a typical hybrid fuel:

$$\dot{r}_h = aG^n, \tag{13}$$

where $\dot{r}_h$ is the burning (regression) rate of the hybrid fuel.

The volumes occupied by dm_o^*, dm_{fo}^* and dm_f are simply obtained by dividing relations (9), (10) and (11) by ρ_f:

$$dV_o^* = \varepsilon 2\pi r L dr; \tag{14}$$

$$dV_{fo}^* = \varepsilon\varphi 2\pi r L dr; \tag{15}$$

$$dV_f = 2\pi r L dr (1-\varepsilon\varphi). \tag{16}$$

As mentioned above, $dV_o^* + dV_{fo}^*$ burns like a solid fuel with the burning speed given by (12) and dV_f burns like a hybrid fuel with a regression speed given by (13).

Using (14), (15) and (16) the average burning rate is obtained for a hybrid fuel doped with an oxidizer:

$$\dot{r}_m = \dot{r}_s\varepsilon(1+\varphi) + \dot{r}_h(1-\varepsilon\varphi), \tag{17}$$

where $\dot{r}_m$ is an average burning rate.

By using (12) and (13) in (17) we get:

$$\dot{r}_m = cp^l\varepsilon(1+\varphi) + aG^n(1-\varepsilon\varphi). \tag{18}$$

Let's assume that $\phi = 1$. This means that the solid oxidizer (which is a dopant for the hybrid fuel) needs an equal amount of solid fuel to oxidizer; in other words the two species are stoichiometrically equal. Results can be obtained in a similar way for $\phi \neq 1$; in this paper $\phi = 1$ is chosen for simplicity.

This assumption turns relation (18) into:

$$\dot{r}_m = aG^n + \varepsilon(2cp^\upsilon - aG^n). \tag{19}$$

As was discussed in the first part of this paper, the ideal mass ratio of methane to liquid oxygen is 1:3, hence the stoichiometric factor would be 1:3.

Further, the solid methane is doped with KNO_3 – solid oxidizer. Similarly, the ideal stoichiometric mass ratio of methane to KNO3 is close to 1:3.

As was mentioned above, the oxidizer particles interact with a given fuel volume around them and that mixture behaves like-a solid fuel. More than that, the combination of solid methane and KNO_3 has a burning rate that is 15 times higher than the burning rate of the combination "solid methane-liquid oxygen":

$$cp^\upsilon \sim 15aG^n. \tag{20}$$

Substituting (20) into (19) and considering a doping ratio with an oxidizer of 6% we obtain:

$$\dot{r}_m \cong 1.983aG^n. \tag{21}$$

Hence for a 6% doping with an oxidizer, the regression speed is theoretically increased almost 2-fold. By varying ε between 0% and 100% it is possible to get an increase of the regression speed by a factor of 1 through 20. If a combination of a solid oxidizer and solid fuel (hybrid) is used that burns more than 15 times faster than typical hybrid fuel, then the maximum factor of raise of the regression speed would be over 20. However, due to practical requirements the doping should be limited to 15–18%, which would basically limit the increase of the regression speed to 5–10 times. Still, this shows a great potential of solving one of the fundamental problems of a hybrid rocket motor that is a low regression rate typical for usual solid fuel/liquid oxidizer combinations.

III. APPLICATION OF METHANE-BASED HYBRID ROCKET MOTORS AS UPPER STAGES

An SM-HRM can be used as an upper stage propulsion unit for suborbital or even orbital launchers. A SM-HRM would provide both a safer and a more economical propulsion unit than the current liquid or solid-based units. Furthermore, being cheaper, this might provide universities and research laboratories

with ample opportunities to launch smaller research payloads. Nevertheless, there is a strong tendency today towards mini-, micro- and even nano- satellites with masses from tens of kg to, as low as, sub-kg. All these satellites are launched using traditional launchers but these endeavours are not very economical. Besides, small satellites are "piggybacks" and this means that they are just extra units carried on the launcher, and there is no guarantee on their final orbit. They are just carried along.

Hence, a dedicated launcher for small satellites would be useful and would open a new window of opportunities impossible to access today.

Equally important is a possibility to design suborbital vehicles that can be used exclusively for research purposes, without any need to rely on military rockets converted to suborbital vectors for research purposes. All these things should make the suborbital and orbital research more accessible to universities and research institutes and, hence, increase the scientific productivity.

The present paper deals with an SM-HRM with the I_{sp} of 300 seconds. In the previous sections it was stated that this I_{sp} is obtainable when solid methane is used as fuel and liquid oxygen as an oxidizer. It is assumed here that the dry mass of the stage is 100 kg and the diameter is 150 mm. The payload mass is 50 kg (half the dead mass). For the aerodynamics we assumed tangent ogive nose-cone for which there is plenty of drag coefficient data published in the aerodynamics literature [17–19].

For the hybrid rocket motor the propellant mass flow is assumed to be 2 kg/s and the total burn time 15 seconds, which gives a total mass for the fuel grain and oxidizer of 30 kg.

The force equation that acts on the upper stage is given below:

$$m\,\vec{a} = \vec{T} + \vec{R} + \vec{G} \qquad (22)$$

where $\vec{T}$ is thrust, $\vec{G}$ is weight and $\vec{R}$ is the drag force. The mass of the upper stage, while the rocket motor is working, is given by:

$$m = m_i - \dot{m} \qquad (23)$$

where m_i is the initial mass and $\dot{m}$ is the propellant mass flow going out of the engine. In the present work this mass flow was assumed to be 2 kg/s.

The above equations can be integrated numerically thus giving various relevant physical quantities of velocity, acceleration, height. All of these quantities are functions of time and are shown in Figs. 6 and 7.

In addition, the burnout velocity of the first stage is considered to be 200 m/s and the burnout altitude 6000 meters. These values are taken to be initial conditions for the numerical integration relevant to the upper stage.
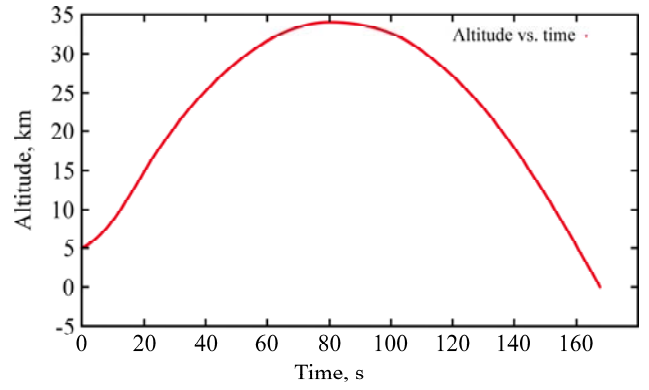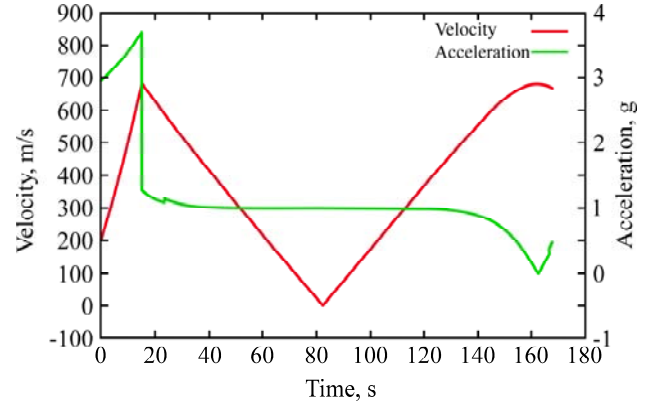

Fig. 6. Altitude vs time.

Fig. 7. Acceleration and velocity vs time.

After the motor burnout of the second stage a discontinuity in acceleration has been observed. This acceleration discontinuity is generally used by onboard computers to command various time-sensitive in-flight operations.

At burnout the maximum velocity is attained simultaneously with the maximum acceleration.

In this case the maximum altitude that the vehicle can reach is ~ 35 km; hence, according to the initial assumptions here, the vehicle can carry a payload of 50 kg to that altitude. This is a considerable payload mass that can accommodate a large variety of high altitude experiments. It is even possible to envisage the usage of the upper stage as a single-stage vehicle, in which case the initial flight conditions would be: altitude 0 meters (ground level) and velocity 0 m/s (it starts from rest). In this case the maximum altitude that the vehicle can reach is lower than in the first case but it still is a considerable altitude. Figure 8 shows the altitude dependence on the flight time for this case.

As was noted above, the entire simulation was started on the assumption of a certain initial dry mass and certain mass for the fuel grain and oxidizer.

As is clear from Fig. 3, there is a dependence of I_{sp} on the chamber pressure. The higher the chamber pressure, the higher the I_{sp}. However, the higher the chamber pressure, the thicker the walls of the chamber should be, and the thicker the walls, the larger the initial dry mass. Increasing the I_{sp} requires an

increase in pressure which in turn leads to an increase in mass (due to increase in thickness of walls). However, the increase in I_{sp}, which leads to a "higher performance" rocket engine, compensates the increase of mass for pressures under a certain optimal value that depends on the specific rocket engine, materials used and the specific geometry of a combustion chamber.
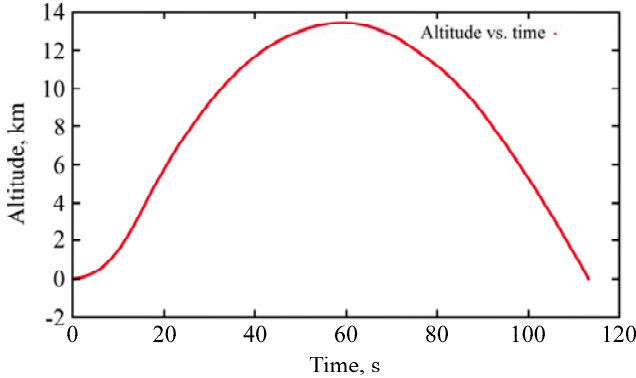

Fig. 8. Altitude one-stage configuration.

Increasing the combustion chamber pressure over the optimal value does indeed increase the I_{sp} but does not increase the overall performance of the launcher. It is assumed here that a relation between the derivatives with respect to the pressure of the I_{sp} and the dry mass should give the optimization criteria and the limit value for the chamber pressure.

By expressing the I_{sp} as a function of pressure it is possible to obtain the derivative of the I_{sp} with respect to the chamber pressure:

$$\frac{dI_{sp}}{dp_c} = \Xi p_c^{2k-1} \chi [1 - (\frac{p_a}{p_c})^{\frac{k-1}{k}}]^{-0.5} \qquad (24)$$

where Ξ, χ and k are coefficients that depend on temperature and chemical properties of the fuel-oxidizer pair, p_c is the chamber pressure and p_a is the atmospheric pressure at the altitude at which the motor operates. Besides, the derivative of the dry mass of the motor with respect to the chamber pressure is given by the following relation:

$$\frac{dm}{dp_c} = \frac{1}{\alpha} \qquad (25)$$

where α is a parameter that depends on the motor diameter D_0, material strength F_{ty} and design safety factor S_D.

The above derivative relations can be used when one needs to optimally design a rocket motor for a certain I_{sp} performance imposed by the flight dynamics requirements.

The above derivatives make it possible to optimize the dry mass and the I_{sp} of a given engine with respect to the combustion pressure. In other words, the above derivatives open a way to finding the optimum operating pressure for a given performance requirement.

IV. CONCLUSIONS

Through the application of oxidizer doping one can obtain a regression speed increase by a factor of 2 to 4. An even higher regression speed increase factor can be obtained by using more advanced oxidizers (e.g., perchlorates, etc.) and a higher doping percentage. There is a maximum limit of the oxidizer doping percentage that can be used for a given O/F pair and it is related to the condition to avoid detonation inside the combustion chamber during the combustion process.

The oxidizer doping widens, in fact, the effective combustion area by allowing two different combustion processes to take place simultaneously thus increasing the apparent regression speed by allowing a more volumetric fuel to be burnt.

This technology can be used on future suborbital and orbital launchers by allowing a higher propulsion performance and a higher launch capability from the same initial launcher mass.

REFERENCES

1. Chiaverini M., Kuo K. *Fundamentals of Hybrid Rocket Combustion and Propulsion.* AIAA, 2007. Vol. 218, 648 p.

2. Asif A. Siddiqi. *The Red Rockets' Glare. Spaceflight and the Russian Imagination, 1857–1957.* New York: Fordham University, 2014. 418 p.

3. Glushko V.P. *Development of Rocket Engineering and Astronautics in the USSR.* M.: Mechanical Engineering, 1987. 304 p.

4. Glushko V.P. *Way to Rocket Engineering.* M.: Mechanical Engineering, 1977. 504 p.

5. Mingireanu F. *Hybrid Rocket Motor Internal Ballistic Model and Oxidizer Doping. Applications. Proceedings of 4th International Conference RAST 2009.* June 2009. P. 198–203.

6. Chelaru T.V., Mingireanu F. Hybrid Rocket Engine, Theoretical Model and Experiment. *Acta Astronautica.* 2011, **68**(11–12), 1891–1902.

7. Collburn B. *A Manual for Hybrid Propulsion System Design.* 1st ed, San Jose, California: Aerocon Systems, 2006. p. 4–40.

8. Sutton G.P., Biblarz O. *Rocket Propulsion Elements.* New York: John Wiley&Sons Inc., 2001., p. 579–606.

9. Laforce P.D. *Technological Development of a Throttling Hybrid Propulsion System.* UTC 2215-FR, January 1967.

10. Dario Pastrone. Approaches to Low Fuel Regression Rate in Hybrid Rocket Engines. *International Journal of Aerospace Engineering.* vol. 2012, Article ID 649753, 12 pages, 2012. doi:10.1155/2012/649753.

11. Chelaru TV; Mingireanu F. Hybrid Rocket Engine, Theoretical Model and Experiment. *Acta Astronautica.* 2011, **68**(11–12), 1891–1902.

12. *Газодинамические основы внутренней баллистики*. Под общ. Ред. К.П. Станюковича. М.: Оборонгиз, 1957. 384 с.

13. Горохов М.С. *Внутренняя баллистика*. Томск: ТГУ, 1943. 243 с.

14. Tsong-Sheng Lee1 and A. Potapkin. *The Performance of a Hybrid Rocket with Swirling GOx Injection*. Technical report published by Defense Technical Information Center, 23 August 2002. 126–132.

15. Christopher P.St.Clair, Rice Eric E., Knuth William H., Gramer Daniel J. *Advanced Cryogenic Solid Hybrid Rocket Engine Developments: Concept and Test Results*. 34th AIAA/ASME/SAE/ASEE Joint propulsion conference & exhibit, July 13–15, 1998, Cleveland, OH, USA: Ft. Belvoir Defence Tehnical Information Center, 1998. Ebook, 10 p.

16. Edward E. Mayo. *Newtonian Aerodynamics for Tangent Ogive Bodies of Revolution*, June, 1965, Goddard Space Flight Center, Greenbelt, Maryland, NASA TM X-55235, NASA Technical Report. 34 p.

17. Wing L.D. Method for Calculating Aerodynamic Heating on Sounding Rocket Tangent Ogive Noses. *Journal of Spacecraft and Rockets*. 1974, **11**(6), 357–362.

18. Butler, Carroll B., Sears, Edward S.; Pallas, Spiros G. *Aerodynamic Characteristics of 2-, 3-, and 4, Caliber Tangent-Ogive Cylinders with Nose Bluffness Ratios of 0.00, 0.25, 0.50, and 0.75 at Mach Numbers from 0.6 to 4.0*, Jan 1977, ADB031340, Air Force Armament Lab Eglin AFB FL. 242 p.

Реферат

В статье представлен инновационный метод увеличения скорости выгорания твердых частиц топлива с помощью добавления присадок в окислитель. Разработана численная модель двигательной установки, дающая в качестве выходных данных параметры производительности. Представлены две модели, которые предсказывают увеличение в 2–3 раза скорости выгорания для вложенных проводов и при добавлении присадки. Кроме того показано, что указанное увеличение скорости выгорания происходит при использовании малых количеств добавок к окислителю, так как есть опасения, что более высокие уровни добавок ведут к неустойчивости горения и детонации. Приводится термохимическая модель для горения с присадкой к окислителю. В этой модели предполагается, что горение происходит вокруг каждой частички окислителя и состоит из двух различных процессов: первый процесс – это горение на поверхности частички твердого топлива, а второй процесс – это горение между твердым топливом и твердым окислителем. Для частицы топлива без присадки горение происходит только на поверхности частицы топлива. Представлены возможные применения соответствующих силовых установок для запуска небольших спутников и описывается одна из них, предназначенная для вывода 50 кг полезного груза на низкую околоземную орбиту (300–500 км над уровнем моря). Предложенные модели основываются на предположении, что использование твердого метана позволит сделать запуск ракеты-носителя экологически чистым.

Ключевые слова: горение, присадки, окислитель, выгорание, баллистика.